Experimental Eye Research 199 (2020) 108183

Contents lists available at ScienceDirect

Experimental Eye Research

journal homepage: www.elsevier.com/locate/yexer

Extrafoveal Müller cells detection in vivo in the human retina: A pilot study based on optical coherence tomography

Alessandro Arrigo [a,*], Cristian Perra [b], Emanuela Aragona [a], Daniele Giusto [b], Claudio Doglioni [c], Luisa Pierro [a], Antonio Giordano Resti [a], Francesco Bandello [a], Maurizio Battaglia Parodi [a]

[a] Department of Ophthalmology, Scientific Institute San Raffaele, Vita-Salute University, Milan, Italy
[b] Department of Electrical and Electronic Engineering (DIEE), CNIT Research Unit, University of Cagliari, Italy
[c] Unit of Pathology, IRCCS San Raffaele Scientific Institute, Milano, Italy

ARTICLE INFO

Keywords:
Müller cells
OCT
In vivo quantification
Post-processing

ABSTRACT

Müller cells (MC) represent a key element for the metabolic and functional regulation of the vertebrate retina. The aim of the present study was to test the feasibility of a new method for the in-vivo detection and quantification of extrafoveal MC in human retina. We developed a new approach to isolate and analyse extrafoveal MC in vivo, starting from structural optical coherence tomography data. Our pilot investigation was based on the optical properties of MC, which are known to not interfere with the light reaching the outer retinal structures. We reconstructed MC in the macular region of 18 healthy subjects and the quantitative analyses revealed ~42,000/9 mm^2 cells detected. Furthermore, we included 2 patients affected by peripheral intraocular melanoma, with macular sparing, needing surgical enucleation. We used these two eyes to perform a qualitative comparison between our reconstructions and histological findings. Our study represents the first pilot investigation dedicated on the non-invasive isolation and quantification of MC, in-vivo, in human retina. Although we are aware that our study has several limitations, first of all related with the proper detection of foveal MC, because of the peculiar z-shape morphology, this approach may open new opportunities for the non-invasive in vivo analysis of MC, providing also potential useful perspectives in retinal diseases.

1. Introduction

Müller cells (MC) play a fundamental role in the metabolic regulation of the vertebrate retina, being the most represented glial cells within retinal structure. Animal histological studies showed that MC number varies from 8000 cells/mm^2 in the periphery to about 15,000 cells/mm^2 in the retinal central region (Reichenbach et al., 1991; Dreher et al., 1992). The ratio between cones and MC is 1:1 in the primate fovea, tending to decrease moving away from the center; this leads to an estimate density of MC > 30,000 cells/mm^2 in the fovea. MC mean length varies from 100 to 300 μm (Distler and Dreher, 1996), reaching up to 1700 μm in the human fovea because of the peculiar z-shape morphology (Bringmann et al., 2018), and are characterized by a single process oriented toward the outer retina and several ramifications oriented toward the inner retina. MC run from the inner limiting membrane (ILM) to the external limiting membrane (ELM), with anatomical relationship with retinal nerve fiber layer (RNFL), ganglion cell layer (GCL), inner plexiform layer (IPL), inner nuclear layer (INL), outer plexiform layer (OPL) and outer nuclear layer (ONL) (Reichenbach and Wohlrab, 1986). MC cover several complex functions including retinal development and metabolic modulation. Moreover, MC have also a role in the reduction of light-scattering phenomena, thus being considered a guide for the light reaching the photoreceptors (Reichenbach and Bringmann, 2013).

In the recent years, optical coherence tomography (OCT) techniques offered the opportunity to perform non-invasively, in vivo, detailed analyses of the human retina, providing comparable data to histological studies. Further details can be achieved by means of post-processing algorithms dedicated to further improve the information provided by light properties of each retinal layer.

The main aim of the present pilot study was to propose a new post-processing technique to detect and analyse MC in the healthy human retina.

* Corresponding author. Department of Ophthalmology, Scientific Institute Ospedale San Raffaele, University Vita-Salute, via Olgettina 60, 20132, Milan, Italy.
E-mail address: alessandro.arrigo@hotmail.com (A. Arrigo).

https://doi.org/10.1016/j.exer.2020.108183
Received 28 April 2020; Received in revised form 27 July 2020; Accepted 3 August 2020
Available online 8 August 2020

2. Material and methods

2.1. Study setting and images acquisitions

The study was designed as a pilot, cross-sectional, observational case series. Consecutive human healthy subjects were enrolled in the Department of Ophthalmology of IRCCS San Raffaele Hospital, Milan, Italy. Moreover, patients with ocular neoplasia, not involving the macular region and requiring surgical enucleation, were also recruited. Exclusion criteria were: age<18 years, any ocular or systemic disease potentially interfering with the results of the study. Each subject and patient provided a signed informed consent before the examination, in accordance with the Declaration of Helsinki. The entire study was approved by the ethical committee of IRCCS San Raffaele Hospital, Milan, Italy.

Overall, 18 healthy subjects (10 men, mean age 35 ± 10 years) were included. Moreover, 2 patients (1 man, mean age 51 ± 9 years) affected by peripheral intraocular melanoma, not involving the macular region, without any other ocular or systemic disorder, and underwent surgical enucleation were analyzed as well.

The imaging protocol included high resolution 3 × 3mm (HxV = 320 × 320) macular OCT angiography (OCTA) acquisitions, obtained by a swept source DRI Triton Topcon device (Topcon Corporation; Tokyo, Japan) (wavelength 1050 nm; 100.000 A-Scans per second; in-depth resolution digital 2.6 μm and optical function 8 μm). Only high-quality images, evaluated by means of the Topcon Quality Index >70, were considered. The following exclusion criteria were adopted: age<18 years old, any ocular or systemic disease potentially affecting the results of the study. The diagnosis of intraocular melanoma was performed by means of a complete ophthalmologic examination, comprehensive of multimodal imaging and ultrasonography. For the patients, any previous treatment and any other systemic disease were considered with exclusion criteria. After the OCTA acquisition and the surgical enucleation, the eye underwent histological assessment. In particular, 3 × 3mm area of the macular region was examined by means of Vimentin and glial fibrillary acidic protein (GFAP), which are considered excellent antibodies for MC detection (Wakakura and Foulds, 1988; Okada et al., 1990; Verardo et al., 2008). In more details, macular samples were fixed in 4% paraformaldehyde for 2 h at 8–10 °C and were processed for immunostaining detection of MC using specific mouse-derived antibodies (ARG30088 Astrocyte Maturation/Muller Cell Marker Antibody Duo; Arigo biolaboratories Corp.). The finally marked samples were cut longitudinally on a cryostat (Leica Microsystems, Nussloch GmbH, Nussloch, Germany), considering 14–20 μm thickness. Macular sections were analyzed by a blinded observer (CD) with the aid of a fluorescence microscope (Leica CTR5500; Leica Microsystems). Representative images were acquired with a confocal microscope (TCS SP5; Leica Microsystems). Thus, the MC morphological representation was compared with OCT imaging.

2.2. Theoretical assumption

The MC detection started with the assumption that extrafoveal MC are vertically oriented elements, not interfering with light passage and absorption. From this point of view, the main scope of the analysis was to isolate from the 3 × 3mm volume the non-reflective vertical signal included between the ILM and ELM. With respect to foveal MC, the peculiar z-shape morphology together with the considerably longer length and the lower thickness, below the resolution limits of current OCT devices, remarkably affected the ability of our algorithm to detect these specific MC. For these reasons, we mainly focused our analyses on extrafoveal MC.

2.3. Muller's cells detection algorithm

This section presents a method for detecting and counting MC in an OCT volume. The method consists in a set of algorithms designed from processing OCT volumes, identifying segments of Muller's cells in the volume, and counting the number of these cells. The proposed architecture is composed of the following blocks: data intermediate format, registration, layer extraction, Müller cells counter.

2.4. Volume registration

The first block is an application program interface (API) between the external data representation (e.g. the data generated by the digital retinal image device) and the internal data representation. The API converts the raw scan and OCTA flow information into the following matrixes of data

$$S(x, y, z) \tag{1}$$

$$F(x, y, z) \tag{2}$$

Adjacent OCT scans are often misaligned resulting in a missing correspondence between adjacent voxels in the z direction. The procedure of spatial alignment of OCT scans is called registration. There exist several algorithms in literature for medical image registration. Considering that the expected width of a Müller cell in the volumetric data is 1 or 2 voxels, it is important to assure that the registration process does not alter the voxel's intensity. With this motivation, a basic algorithm based only on rigid translation is adopted.

From the scan volume, a threshold is computes as

$$t = a \cdot mean(S(x, y)) \tag{3}$$

where a is a parameter used for adapting the threshold level to the different statistics of OCT data. The scan volume is then thresholded as follows

$$S^{'}(x, y, z) = \begin{cases} S(x, y, z) & S(x, y, z) \geq t \\ 0 & S(x, y, z) < t \end{cases} \tag{4}$$

The barycenter $\boldsymbol{b} = (b_x, b_y, b_z)$ computed from $S^{'}(x, y, z)$ is then used for a rigid translation of the per-slice barycenter $\boldsymbol{b}_{xy}(z)$ to the baricenter $\boldsymbol{b}$. Finally, the best motion vector between adjacent slices is calculated constrained by the minimization of the mean square error. The motion vector search area is controlled by the two parameters Δx, and Δy, for the full search area $[-\Delta x, \Delta x] \times [-\Delta y, \Delta y]$. The same translations are applied to corresponding frames in the OCTA flow volume F (x,y,z).

2.4.1. OCT layer detection

The layer detection process is composed of several steps. A slice from the OCT volume is thresholded using the Otsu's methods (Otsu, 1979). Then a sequence of morphological transformation is applied for obtaining a clean mask of the region of interest. These steps are erosion, closing, filling, removing small unconnected regions, and cleaning the left and right sides of the image.

Finally, a top edge detection is applied for determining the ILM edge, RPE edge, and ELM edge.

2.5. Müller cell filter

The Müller density defined an algorithm that jointly analyses the OCT scan and the OCTA flow information. The main idea is to classify each voxel with a confidence parameter for the voxel being part of a Müller cell.

2.6. The main assumptions are as follows

A1) MC are present in the volume between ILM and ELM edges;
A2) MC are represented as monotonic piecewise linear functions;
A3) MC in OCT scan have very low intensity;
A4) MC are not present where OCTA flow is very active;

A5) MC are organized as smooth lines without abrupt changes of direction. From these assumptions we can model a Müller cell filter as follows.

(A1) A mask is applied to the scan and OCTA flow information in order to extract only voxels between ILM and ELM edges. We denote these voxels as Müller scan (S_m) and OCTA flow (F_m) volumes:

$$S_m(x,y,z) \subset S(x,y,z),\ where\ (x,y,z)\ between\ ILM\ and\ ELM\ edges \quad (5)$$

$$F_m(x,y,z) \subset F(x,y,z),\ where\ (x,y,z)\ between\ ILM\ and\ ELM\ edges \quad (6)$$

(A2) A set of 3D matched filter representing 3D segments of length L at different orientations are then applied to the Müller volumes. The filter giving the highest response (Q_m (x,y,z)) will signal that the corresponding voxel is part of a 3D segment having a given orientation (D_m (x,y,z)).

$$Q_m(x,y,z) = max\ S_m(x,y,z)*M_i(x,y,z), \forall i \quad (7)$$

$$D_m(x,y,z) = argmax_i\ S_m(x,y,z)*M_i(x,y,z), \forall i \quad (8)$$

(A3) A threshold t_s is defined for filtering out voxels with low response

$$Q_m(x,y,z) = 0,\ where\ Q_m(x,y,z) < t_s \quad (9)$$

(A4) An OCTA flow threshold t_f is defined for filtering out voxels with high flow levels

$$Q_m(x,y,z) = 0,\ where\ F_m(x,y,z) > t_f \quad (10)$$

2.7. Müller cell detection and quantification

A region growing approach is proposed for extracting the MC from the Müller volume. At first, a percentage p of the voxels with the highest response Q_m (x,y,z) to the Müller filter are extracted for being used as seeds for the region growing process of the Müller cells. Then neighboring pixels of seed voxels are added to the region in decreasing order of magnitude Q_m. For each Müller voxel, the region growing area is a double cone, i.e. two cones placed apex to apex. This constraint, motivated by assumption A5, for the region growing process to evolve with smooth changes of directions. This process generates a set of N lines which are the detected Müller cells.

The quantitative analysis of MC was performed considering only the single lines localized at the level of the outer nuclear layer, in order to reduce the risk of oversampling secondary to the presence of possible ramifications detected al the level of the inner retinal layers. The entire macular volume of 3 × 3mm was considered for the MC quantification.

3. Results

Best corrected visual acuity was 0.0 ± 0.0 LogMAR (20/20 Snellen equivalent) for all subjects and patients.

Our analyses allowed to evaluate and isolate, from structural OCT images, the trans-retinal, vertical, linear, hyporeflective signal, included between the ILM and the ELM (Fig. 1). This signal was characterized by a continuous "single-line" morphology. Remarkably, the signal disclosed by structural OCT images qualitatively matched with the histological results obtained after the treatment of the enucleated tissue with Vimentin and GFAP (Fig. 2). It is worth of notice a different amount of MC signal, disclosed by structural OCT, and resulting more detectable in the extrafoveal region than in foveal one (Fig. 3).

The quantitative analysis of MC, performed considering the signal detected at the level of the outer nuclear layer, showed an overall number of MC corresponding to 42232 ± 3478 cells localized in the macular volume of 3 × 3mm (~42,000/9 mm^2 cells) (Table 1).

4. Discussion

Müller cells represent a fundamental cytotype in the animals and human retina, due to the high number of regulatory functions performed (Dreher et al., 1992; Reichenbach and Bringmann, 2020). MC are also characterized by the role of providing a low-scattering passage for the light reaching OPL/ONL border, thus mediating the image transfer through the retina with minimal distortion and low light loss (Franze et al., 2007). This was true for the peripheral retinal regions; with respect to the macula, turning to be thicker than the rest of the retina, this specific role of the MC is just secondary, since light scattering phenomena are less pronounced. In this case, considering the extremely high concentration of MC in the macular region, it is assumable that these specific MC cover other fundamental metabolic and regulatory roles, thus increasing the concept of MC as a major multifunctional component of the vertebrate retina (Bringmann et al., 2018; Reichenbach and Bringmann, 2020). We started from these evidences to make our assumption that MC may correspond to vertically oriented, trans-retinal, hyporeflective signal on structural OCT. On the basis of this theory, we were able to extrapolate this hyporeflective, continuous, trans-retinal signal from the macular structural OCT horizontal scans. In order to provide a kind of comparison with histological data, we

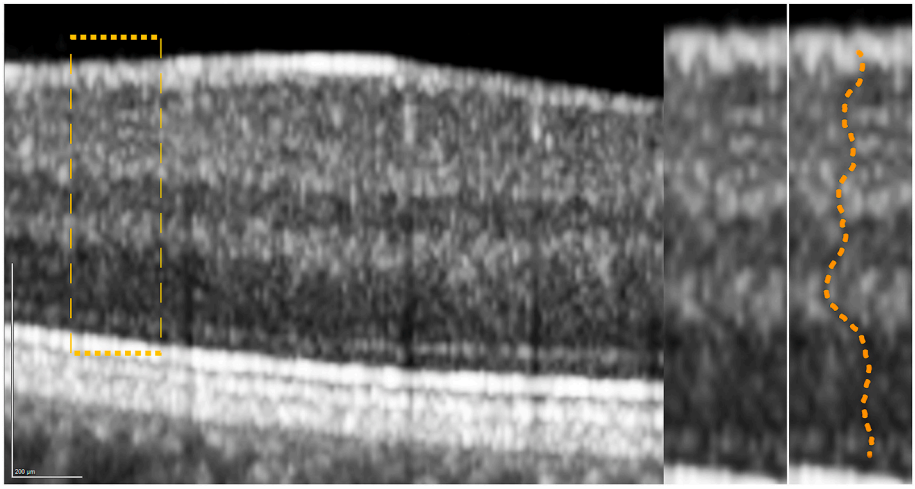

Fig. 1. Structural OCT signal interpreted as Müller cells. From original structural OCT image, it is possible to clearly distinguish vertical, trans-retinal, linear, hyporeflective signals, contained between ILM and ELM. A magnified section is shown in the right part of the figure, where we manually highlighted a single extrafoveal MC signal (orange line). (For interpretation of the references to colour in this figure legend, the reader is referred to the Web version of this article.)

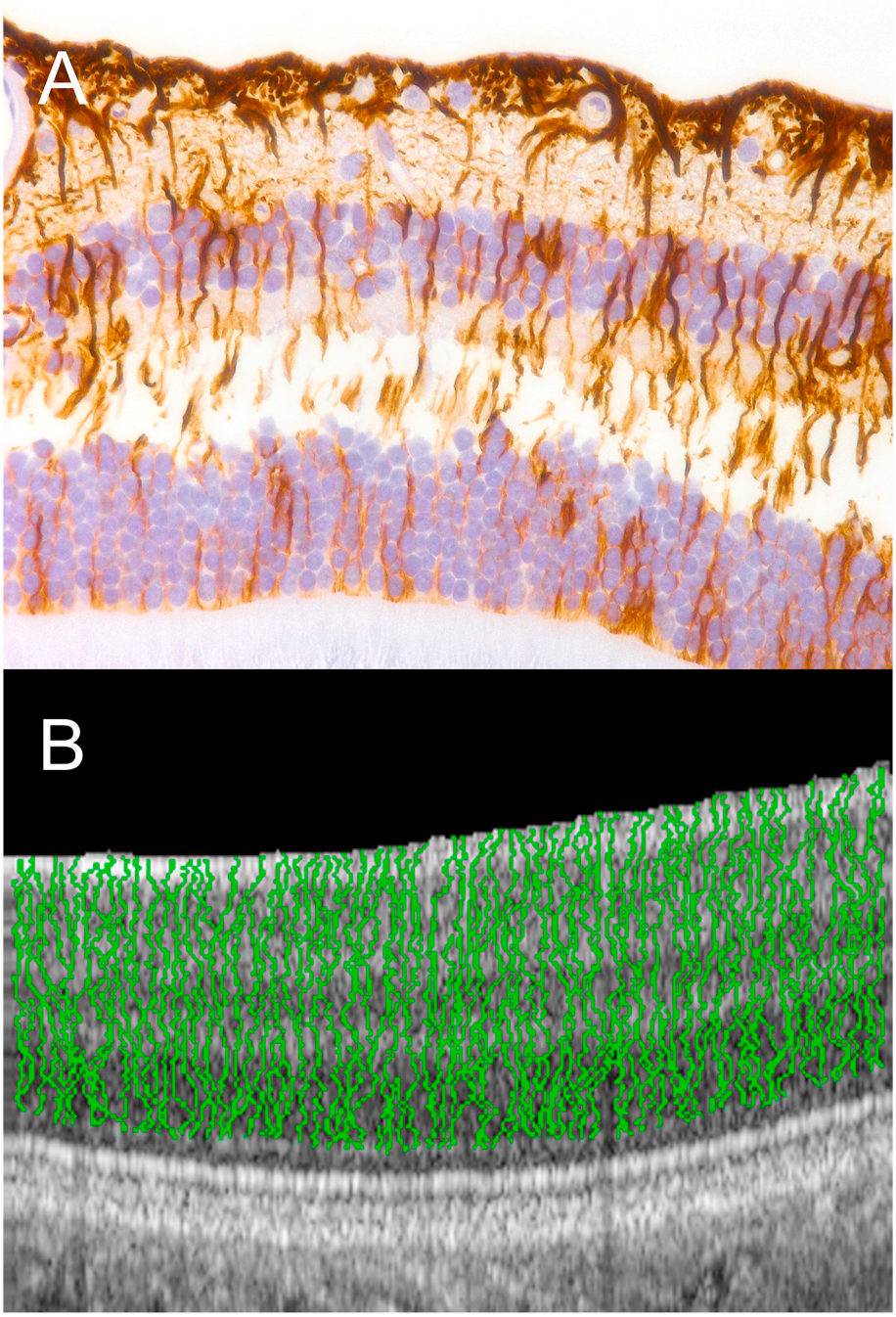

Fig. 2. Müller cells detection on histological analysis after tissue treatment with Vimentin and GFAP (A) and Müller cells detection based on structural OCT analyses (B) in the same eye. The structural OCT reconstruction represents a multiple-slabs reconstruction, selected to represent MC as continuous linear trans-retinal signal, in order to make clearer the visualization of the MC.

included into our analyses also two patients needing surgical enucleation, with macular sparing. Remarkably, the isolated structural OCT signal, which we interpreted as MC, showed good matching with our histological data. Moreover, the overall number of macular MC partially agrees with previous histological quantifications (Distler and Dreher, 1996). However, the intrinsic resolution limitations of current structural OCT devices make challenging the identification of structures under 8 μm of size. Since the mean diameter of MC is approximatively of 10 μm (range 6–14 μm obtained in Guinea pig) (Agte et al., 2011), and also further thinner in human retina, because of the very high concentration of MC within the fovea (Reichenbach and Bringmann, 2020), it is assumable an underestimation of MC number affecting our study, which should be considered just a first pilot investigation. Similarly, an evident underestimation regarded the different amount of MC signal, detectable in the foveal and extrafoveal region of structural OCT images. In particular, MC signal resulted remarkably less detected at the level of the fovea than in the extrafoveal regions. We might advance two different hypotheses to explain this finding. The first one is related with resolution limitations, making current structural OCT images not sufficient to detect foveal MC. These result more numerous within the fovea than in the rest of the retina, thus making assumable MC sizes below the 8 μm threshold of structural OCT sensitivity. Moreover, MC show a very peculiar anatomy at the level of the fovea (Reichenbach and Bringmann, 2020), following a z-shape morphology, making possible the change of their optical properties and interfering with their proper detection through our approach.

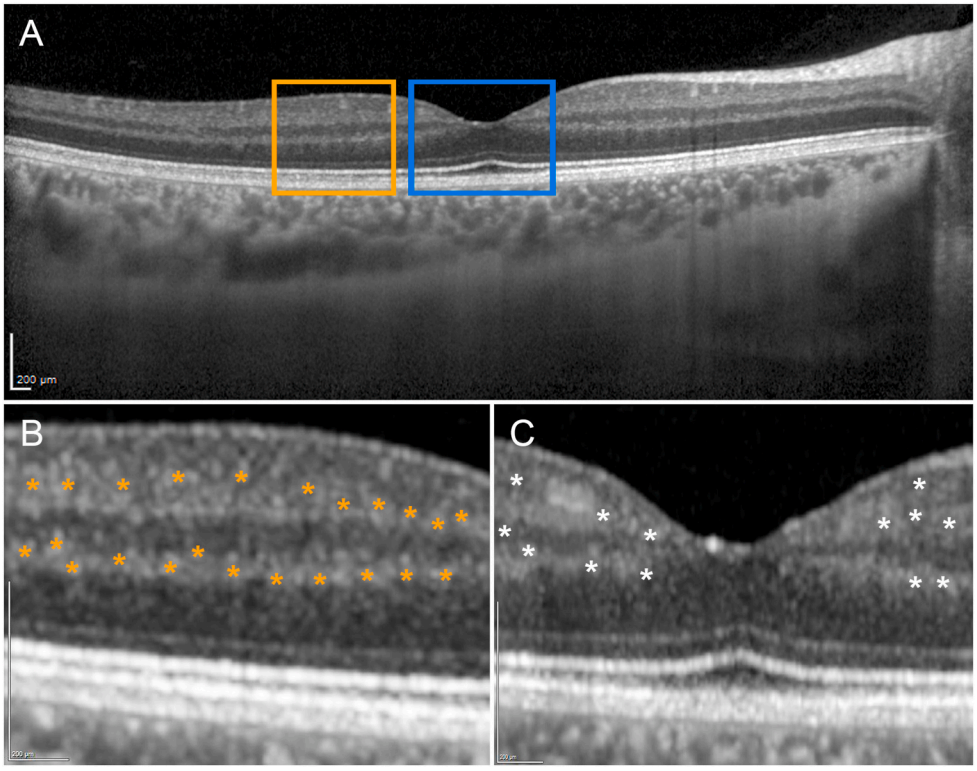

Fig. 3. Müller cells signal detection on structural OCT. MC signal detection varies in accordance with the distance from the fovea. In particular, starting from the entire structural OCT horizontal line (A), the extrafoveal region (orange square and magnified B) shows high amount of MC signal (marked by orange asterisks). On the contrary, the foveal region (blue square and magnified C) discloses remarkably lower MC signal (marked by white asterisks). (For interpretation of the references to colour in this figure legend, the reader is referred to the Web version of this article.)

Table 1
Müller cells quantification, in vivo, in healthy eyes.

Müller Cells Quantification	
Subject 1	39673
Subject 2	39695
Subject 3	47312
Subject 4	48622
Subject 5	39949
Subject 6	43209
Subject 7	43639
Subject 8	44686
Subject 9	41421
Subject 10	41152
Subject 11	49770
Subject 12	41624
Subject 13	38439
Subject 14	39047
Subject 15	41626
Subject 16	44491
Subject 17	42842
Subject 18	37719
Subject 19	37115
Subject 20	42614
Min	37115
Max	49770
Mean	42232
Standard deviation	3478

On the other side, the histological quantification of the MC is really challenging too, and it was previously mainly performed in animals' retina, thus making the quantitative values available in the current literature just indicative, rather than precise reference values. It is worth of notice that Bringmann et al. (2018) provided a reference value of foveal MC density in humans, correspondent to around 15000 cells/mm^2. The discrepancy between this value and those reported in our study may be considered the direct consequence of the resolution limits of the current OCT devices, allowing to detect just one part of the entire macular MC together with the already limitation related with the z-shape morphology of foveal MC. Moreover, in order to make our quantification more rigorous, we performed our analyses by counting only the signal isolated at the level of the outer nuclear layer, without the possible overestimation caused by the influence of spurious signal at the level of the inner retina. Since MC histological quantification may be done in different ways and can be affected by several limitations (Taylor and Levenson, 2006; Walker, 2006), it is very difficult to make reliable comparisons with our findings. With respect to MC selective detection, this can be affected by some limitations, including, first of all, the possible inclusion of other retinal cytotypes which might have similar reflectivity signal. We tried to reduce this kind of bias by isolating only continuous trans-retinal signal; however, we cannot exclude at all the possible presence of other retinal elements in our analyses. Another attempt to reduce possible biases was the usage of blood flow information through OCTA. In particular, we excluded all retinal voxels resulted positive after the decorrelation signal analysis, thus being interpretable as intraretinal vessels.

Considering the well-known involvement of MC in retinal diseases (Bringmann and Wiedemann, 2012), as well as their involvement in retinal regenerative phenomena (Goldman, 2014), the perspective of MC quantification in vivo may open new frontiers for the diagnosis and treatment of retinal diseases.

We are aware that the present investigation should be considered only a pilot study, conducted with a low number of subjects, affected by several limitations related with the experimental methods, as above discussed, and also related with intrinsic limitations of imaging techniques (Spaide et al., 2015, 2018). Moreover, we would highlight that our approach is limited to image resolution $\geq$8 µm, thus making possible to detect just one part of the entire information. Furthermore, the current approach is poorly sensitive to foveal MC for two main reasons. The first one is related with the extremely high density of foveal MC, which resulted more compacted and thinner than in the rest of the retina. In addition, the z-shape morphology of foveal MC may strongly alter their optical properties, making difficult the proper isolation through our algorithm. For these reasons, we are aware that the future improvements of OCT devices resolution and the development of a dedicated algorithm

for the z-shape profile definition would overcome this current limitation, which affects also the quantification of MC. The future application of this kind of quantitative approaches on even more advanced structural OCT devices will help to increase the amount of information available through these imaging methodologies. Furthermore, we provided few histological findings just to make a qualitative assessment, but we could not perform any kind of quantitative comparative analysis, due to the inclusion of only two eyes both with imaging and histological data.

In conclusion, our pilot investigation proposed a new post-processing method to analyse in vivo MC, in human retina. Further larger studies are warranted to support our preliminary findings and to assess the possible application in retinal diseases.

Financial support

None.

Financial disclosures

Francesco Bandello consultant for: Alcon (Fort Worth, Texas, USA), Alimera Sciences (Alpharetta, Georgia, USA), Allergan Inc (Irvine, California, USA), Farmila-Thea (Clermont-Ferrand, France), Bayer Shering-Pharma (Berlin, Germany), Bausch And Lomb (Rochester, New York, USA), Genentech (San Francisco, California, USA), Hoffmann-La-Roche (Basel, Switzerland), NovagaliPharma (Évry, France), Novartis (Basel, Switzerland), Sanofi-Aventis (Paris, France), Thrombogenics (Heverlee, Belgium), Zeiss (Dublin, USA). All other authors have no disclosures to declare.

Declaration of competing interest

None.

Acknowledgements

None.

References

Agte, S., Junek, S., Matthias, S., Ulbricht, E., Erdmann, I., Wurm, A., Schild, D., Käs, J.A., Reichenbach, A., 2011. Müller glial cell-provided cellular light guidance through the vital Guinea-pig retina. Biophys. J. 101 (11), 2611–2619.

Bringmann, A., Wiedemann, P., 2012. Müller glial cells in retinal disease. Ophthalmologica 227 (1), 1–19.

Bringmann, A., Syrbe, S., Görner, K., Kacza, J., Francke, M., Wiedemann, P., Reichenbach, A., 2018. The primate fovea: structure, function and development. Prog. Retin. Eye Res. 66, 49–84.

Distler, C., Dreher, Z., 1996. Glia cells of the monkey retina–II. Müller cells. Vis. Res. 36 (16), 2381–2394.

Dreher, Z., Robinson, S.R., Distler, C., 1992. Müller cells in vascular and avascular retinae: a survey of seven mammals. J. Comp. Neurol. 323 (1), 59–80.

Franze, K., Grosche, J., Skatchkov, S.N., Schinkinger, S., Foja, C., Schild, D., Uckermann, O., Travis, K., Reichenbach, A., Guck, J., 2007. Muller cells are living optical fibers in the vertebrate retina. Proc. Natl. Acad. Sci. U. S. A. 104 (20), 8287–8292.

Goldman, D., 2014. Müller glial cell reprogramming and retina regeneration. Nat. Rev. Neurosci. 15 (7), 431–442.

Okada, M., Matsumura, M., Ogino, N., Honda, Y., 1990. Müller cells in detached human retina express glial fibrillary acidic protein and vimentin. Graefes Arch. Clin. Exp. Ophthalmol. 228 (5), 467–474.

Otsu, N., 1979. A threshold selection method from gray-level histograms. IEEE Transactions on Systems, Man, and Cybernetics 9 (1), 62–66.

Reichenbach, A., Bringmann, A., 2013. New functions of Müller cells. Glia 61 (5), 651–678.

Reichenbach, A., Bringmann, A., 2020. Glia of the human retina. Glia 68 (4), 768–796.

Reichenbach, A., Schnitzer, J., Friedrich, A., Knothe, A.K., Henke, A., 1991. Development of the rabbit retina: II. Müller cells. J. Comp. Neurol. 311 (1), 33–44.

Reichenbach, A., Wohlrab, F., 1986. Morphometric parameters of Müller (glial) cells dependent on their topographic localization in the nonmyelinated part of the rabbit retina. A consideration of functional aspects of radial glia. J. Neurocytol. 15 (4), 451–459.

Spaide, R.F., Fujimoto, J.G., Waheed, N.K., 2015. Image artifacts in optical coherence tomography angiography. Retina 35 (11), 2163–2180.

Spaide, R.F., Fujimoto, J.G., Waheed, N.K., Sadda, S.R., Staurenghi, G., 2018. Optical coherence tomography angiography. Prog. Retin. Eye Res. 64, 1–55.

Taylor, C.R., Levenson, R.M., 2006. Quantification of immunohistochemistry–issues concerning methods, utility and semiquantitative assessment II. Histopathology 49 (4), 411–424.

Verardo, M.R., Lewis, G.P., Takeda, M., Linberg, K.A., Byun, J., Luna, G., Wilhelmsson, U., Pekny, M., Chen, D.F., Fisher, S.K., 2008. Abnormal reactivity of muller cells after retinal detachment in mice deficient in GFAP and vimentin. Invest. Ophthalmol. Vis. Sci. 49 (8), 3659–3665.

Wakakura, M., Foulds, W.S., 1988. Immunocytochemical characteristics of Müller cells cultured from adult rabbit retina. Invest. Ophthalmol. Vis. Sci. 29 (6), 892–900.

Walker, R.A., 2006. Quantification of immunohistochemistry–issues concerning methods, utility and semiquantitative assessment I. Histopathology 49 (4), 406–410.